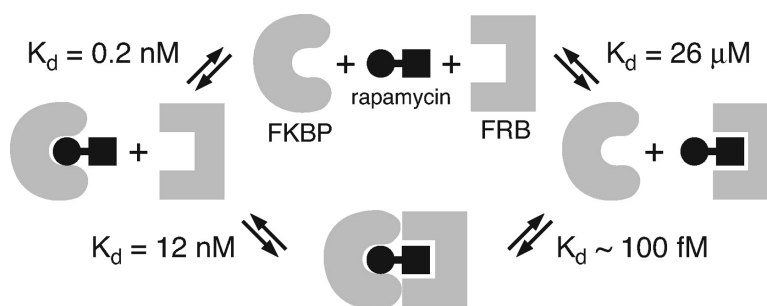


## Characterization of the FKBP·Rapamycin·FRB Ternary Complex

Laura A. Banaszynski, Corey W. Liu, and Thomas J. Wandless

*J. Am. Chem. Soc.*, **2005**, 127 (13), 4715-4721 • DOI: 10.1021/ja043277y • Publication Date (Web): 09 March 2005

Downloaded from <http://pubs.acs.org> on March 25, 2009



### More About This Article

Additional resources and features associated with this article are available within the HTML version:

- Supporting Information
- Links to the 13 articles that cite this article, as of the time of this article download
- Access to high resolution figures
- Links to articles and content related to this article
- Copyright permission to reproduce figures and/or text from this article

[View the Full Text HTML](#)

## Characterization of the FKBP·Rapamycin·FRB Ternary Complex

Laura A. Banaszynski,<sup>‡</sup> Corey W. Liu,<sup>†</sup> and Thomas J. Wandless\*<sup>‡</sup>

Contribution from the Department of Chemistry, Stanford Magnetic Resonance Laboratory, and Department of Molecular Pharmacology, Stanford University, Stanford, California 94305

Received November 8, 2004; E-mail: wandless@stanford.edu

**Abstract:** Rapamycin is an important immunosuppressant, a possible anticancer therapeutic, and a widely used research tool. Essential to its various functions is its ability to bind simultaneously to two different proteins, FKBP and mTOR. Despite its widespread use, a thorough analysis of the interactions between FKBP, rapamycin, and the rapamycin-binding domain of mTOR, FRB, is lacking. To probe the affinities involved in the formation of the FKBP·rapamycin·FRB complex, we used fluorescence polarization, surface plasmon resonance, and NMR spectroscopy. Analysis of the data shows that rapamycin binds to FRB with moderate affinity ( $K_d = 26 \pm 0.8 \mu\text{M}$ ). The FKBP12·rapamycin complex, however, binds to FRB 2000-fold more tightly ( $K_d = 12 \pm 0.8 \text{nM}$ ) than rapamycin alone. No interaction between FKBP and FRB was detected in the absence of rapamycin. These studies suggest that rapamycin's ability to bind to FRB, and by extension to mTOR, in the absence of FKBP is of little consequence under physiological conditions. Furthermore, protein–protein interactions at the FKBP12–FRB interface play a role in the stability of the ternary complex.

### Introduction

Rapamycin (Figure 1A) is a 31-membered macrolide anti-fungal antibiotic that was first isolated from *Streptomyces hygroscopicus* in an Easter Island soil sample in 1975.<sup>1–4</sup> Interest in the compound intensified in 1987, following the discovery of FK506, a potent immunosuppressant with striking structural similarity.<sup>5</sup> Rapamycin binds with high affinity ( $K_d = 0.2 \text{nM}$ ) to the 12-kDa FK506 binding protein (FKBP12, hereafter called FKBP)<sup>6–8</sup> as well as to a 100-amino acid domain (E2015 to Q2114) of the mammalian target of rapamycin (mTOR) known as the FKBP–rapamycin binding domain (FRB).<sup>9–12</sup> Rapamycin is an FDA-approved drug which is used clinically as an immunosuppressant for organ transplant patients. Rapamycin is also important scientifically, as it is a potent and

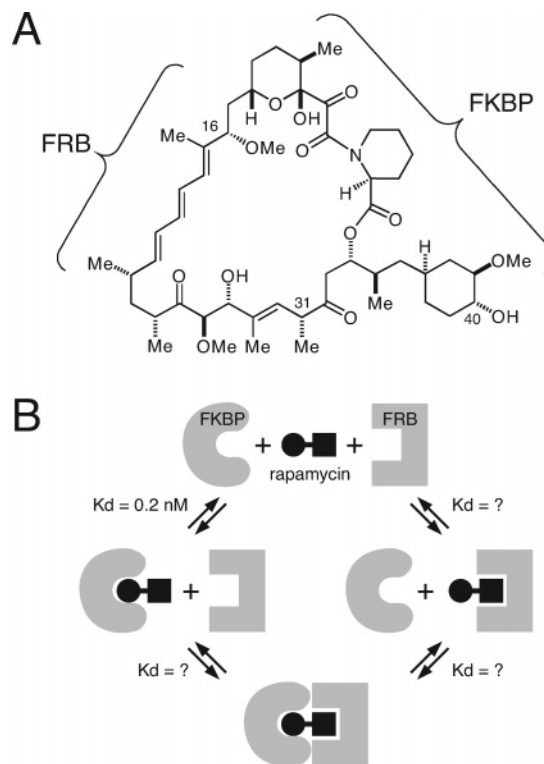


**Figure 1.** (A) Chemical structure of rapamycin showing the FKBP and FRB binding domains. (B) Schematic diagram representing the four possible binding events involved in the formation of the FKBP·rapamycin·FRB ternary complex.

specific inhibitor of mTOR, which has been shown to be a major effector of cell growth and proliferation via the regulation of protein synthesis. Due to this activity, the mTOR pathway is

<sup>‡</sup> Department of Chemistry.

<sup>†</sup> Stanford Magnetic Resonance Laboratory.

<sup>‡</sup> Department of Molecular Pharmacology.

- (1) Vézina, C.; Kudelski, A.; Sehgal, S. N. *J. Antibiot.* **1975**, *28*, 721–726.
- (2) Sehgal, S. N.; Baker, H.; Vézina, C. *J. Antibiot.* **1975**, *28*, 727–732.
- (3) Swindells, D. C. N.; White, P. S.; Findlay, J. A. *Can. J. Chem.* **1978**, *56*, 2491–2492.
- (4) Findlay, J. A.; Radics, L. *Can. J. Chem.* **1980**, *58*, 579–590.
- (5) Tanaka, H.; Kuroda, A.; Marusawa, H.; Hatanaka, H.; Kino, T.; Goto, T.; Hashimoto, M. *J. Am. Chem. Soc.* **1987**, *109*, 5031–5033.
- (6) Siekierka, J. J.; Hung, S. H. Y.; Poe, M.; Lin, C. S.; Sigal, N. H. *Nature* **1989**, *341*, 755–757.
- (7) Harding, M. W.; Galat, A.; Uehling, D. E.; Schreiber, S. L. *Nature* **1989**, *341*, 758–760.
- (8) Bierer, B. E.; Mattila, P. S.; Standaert, R. F.; Herzenberg, L. A.; Burakoff, S. J.; Crabtree, G.; Schreiber, S. L. *Proc. Natl. Acad. Sci. U.S.A.* **1990**, *87*, 9231–9235.
- (9) Brown, E. J.; Albers, M. W.; Shin, T. B.; Ichikawa, K.; Keith, C. T.; Lane, W. S.; Schreiber, S. L. *Nature* **1994**, *369*, 756–758.
- (10) Chiu, M. L.; Katz, H.; Berlin, V. *Proc. Natl. Acad. Sci. U.S.A.* **1994**, *91*, 12574–12578.
- (11) Sabatini, D. M.; Erdjument-Bromage, H.; Lui, M.; Tempst, P.; Snyder, S. H. *Cell* **1994**, *78*, 35–43.
- (12) Chen, J.; Zheng, X. F.; Brown, E. J.; Schreiber, S. L. *Proc. Natl. Acad. Sci. U.S.A.* **1995**, *92*, 4947–4951.

emerging as a critical player in cancer and other metabolic diseases, including diabetes and obesity.<sup>13</sup>

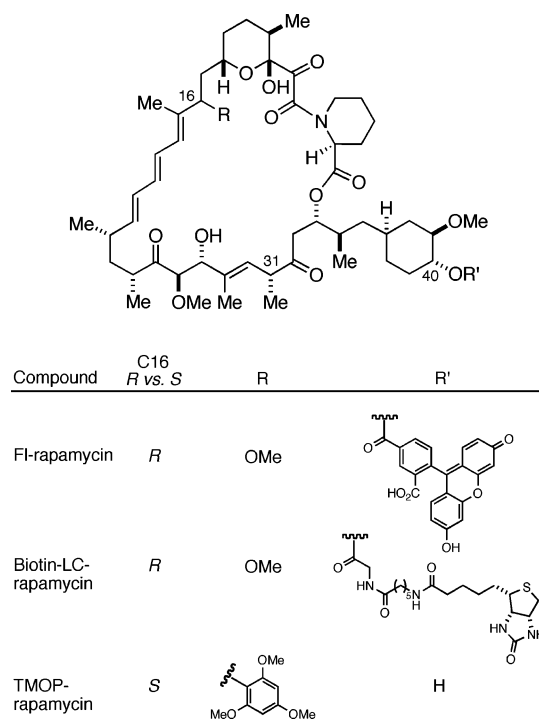
Perhaps the most widespread use of rapamycin has been in technology developed to take advantage of the small molecule's ability to heterodimerize proteins. Proteins of interest can be expressed as fusions to FKBP or FRB, and then conditionally dimerized by the addition of rapamycin.<sup>14–18</sup> This approach has been used to regulate protein expression,<sup>19–21</sup> protein splicing,<sup>22</sup> and glycosylation,<sup>23</sup> to name a few examples.

While a great deal of structural information about the FKBP•rapamycin•FRB ternary complex exists,<sup>24,25</sup> a thorough biophysical analysis of these interactions is lacking. The interaction between FKBP and rapamycin has been well characterized ( $K_d = 0.2$  nM),<sup>8</sup> and early experiments suggest that formation of a ternary complex including FRB is quite favorable ( $K_d \approx 2.5$  nM).<sup>12</sup> These studies also showed that FKBP and FRB do not interact in the absence of rapamycin. Analysis of the crystal structure shows extensive interactions between rapamycin and its two protein partners, but relatively limited interactions between the proteins themselves. Experiments in yeast have shown that FKBP knockouts show resistance to rapamycin,<sup>26,27</sup> and from these experiments it has been postulated that rapamycin cannot bind to mTOR in the absence of FKBP. An alternative explanation is that rapamycin binds to mTOR in the absence of FKBP, but that FKBP is needed to block a protein–protein interaction between mTOR and a critical partner protein. To provide evidence to distinguish between these two possibilities, and to determine if protein–protein interactions contribute to overall complex stability, we sought to characterize the interactions between rapamycin and FRB in the presence and in the absence of FKBP (Figure 1B).

## Results and Discussion

**Fluorescence Polarization Assays.** The crystal structure of the ternary complex shows the C40-cyclohexyl hydroxyl group of rapamycin to be distant from FRB.<sup>24</sup> Therefore, we chose to modify this location when synthesizing fluorescein-rapamycin (Fl-rap, Chart 1) as a tracer for fluorescence polarization experiments. The affinity of Fl-rap for FRB was determined using a standard saturation binding experiment. A fixed concentration of Fl-rap was incubated with various concentrations of FRB, and formation of the Fl-rap•FRB complex was quantitated using an increase in polarization units. An equilib-

Chart 1. Chemical Structures of Rapamycin Derivatives



rium binding analysis of the data gave a dissociation constant of  $490 \pm 39$  nM (Figure 2A).

A competition binding experiment was then performed in order to determine the affinity of unmodified rapamycin for FRB (Figure 2B). FRB and Fl-rap were allowed to associate, and various concentrations of rapamycin were added to compete Fl-rap from the FRB binding pocket, which was measured as a decrease in polarization units. However, the solubility of rapamycin in this buffer (PBS pH 7.4, 0.011% Triton X-100, 1% EtOH) is limited ( $\sim 10$   $\mu$ M), and this fact, coupled with our observation that rapamycin's affinity for FRB is weaker than that of Fl-rap, meant that we could not achieve concentrations of rapamycin necessary to fully compete Fl-rap from FRB. The enhanced affinity of Fl-rap for FRB relative to that of rapamycin for FRB is perhaps due to a combination of rapamycin•FRB binding along with nonspecific binding of the aromatic fluorophore to the hydrophobic protein. The partial competition data were fit using a mathematical model that explicitly considers all species present at equilibrium using ratios of rate constants for association and dissociation of all possible complexes and a corresponding collection of partial differential rate equations from which dissociation constants can be derived.<sup>28</sup> The best fit of the incomplete competition data suggested a dissociation constant of  $5.2$   $\mu$ M ( $R^2 = 0.65$ ) for the affinity of rapamycin for FRB.

The composite surface of the FKBP•rapamycin complex is thought to possess a tighter affinity for FRB relative to rapamycin alone. To test this hypothesis, we repeated the competition binding assay in the presence of FKBP. This competition could not be completed, not due to rapamycin solubility issues but because addition of the fluorescein moiety does not completely abrogate binding of Fl-rap to FKBP (Figure S1, Supporting Information). However, a mathematical

- (13) Hay, N.; Sonenberg, N. *Genes Dev.* **2004**, *18*, 1926–1945.  
 (14) Pollock, R.; Clackson, T. *Curr. Opin. Biotechnol.* **2002**, *13*, 459–467.  
 (15) Clemons, P. A. *Curr. Opin. Chem. Biol.* **1999**, *3*, 112–115.  
 (16) Muthuswamy, S. K.; Gilman, M.; Brugge, J. S. *Mol. Cell. Biol.* **1999**, *19*, 6845–6857.  
 (17) Otto, K. G.; Jin, L.; Spencer, D. M.; Blau, C. A. *Blood* **2001**, *97*, 3662–3664.  
 (18) Janse, D. M.; Crosas, B.; Finley, D.; Church, G. M. *J. Biol. Chem.* **2004**, *279*, 21415–21420.  
 (19) Ho, S. N.; Biggar, S. R.; Spencer, D. M.; Schreiber, S. L.; Crabtree, G. R. *Nature* **1996**, *382*, 822–826.  
 (20) Rivera, V. M.; Clackson, T.; Natesan, S.; Pollock, R.; Amara, J. F.; Keenan, T.; Magari, S. R.; Phillips, T.; Courage, N. L.; Cerasoli, F.; Holt, D. A.; Gilman, M. *Nat. Med.* **1996**, *2*, 1028–1032.  
 (21) Schlatter, S.; Senn, C.; Fussenegger, M. *Biotechnol. Bioeng.* **2003**, *83*, 210–225.  
 (22) Mootz, H. D.; Blum, E. S.; Tyszkiewicz, A. B.; Muir, T. W. *J. Am. Chem. Soc.* **2003**, *125*, 10561–10569.  
 (23) Kohler, J. J.; Bertozzi, C. R. *Chem. Biol.* **2003**, *10*, 1303–1311.  
 (24) Choi, J.; Chen, J.; Schreiber, S. L.; Clardy, J. *Science* **1996**, *273*, 239–242.  
 (25) Liang, J.; Choi, J.; Clardy, J. *Acta Crystallogr.* **1999**, *D55*, 736–744.  
 (26) Heitman, J.; Movva, N. R.; Hall, M. N. *Science* **1991**, *253*, 905–909.  
 (27) Koltin, Y.; Faucette, L.; Bergsma, D. J.; Levy, M. A.; Caffferkey, R.; Koser, P. L.; Johnson, R. K.; Livi, G. P. *Mol. Cell. Biol.* **1991**, *11*, 1718–1723.

- (28) Braun, P. D.; Wandless, T. J. *Biochemistry* **2004**, *43*, 5406–5413.

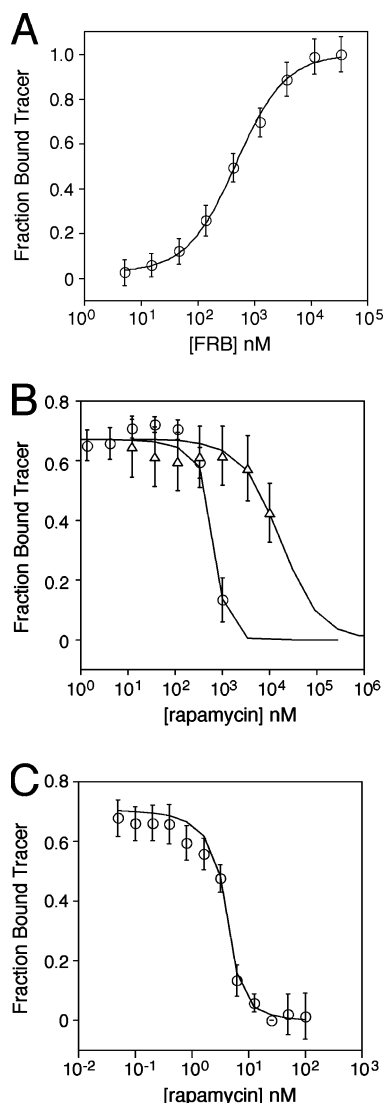


**Figure 2.** Fluorescence polarization assays. (A) A saturation binding experiment between 2 nM FI-rap and various concentrations of FRB indicate a dissociation constant of  $490 \pm 39$  nM. (B) Competition binding experiments show the affinity of rapamycin for FRB in the presence (circles) and absence (triangles) of FKBP. (C) Competition binding experiment shows the affinity of rapamycin for FKBP ( $K_d = 0.35$  nM,  $R^2 = 0.96$ ).

fit of the competition data, using a rapamycin·FRB primary dissociation constant of  $5.2 \mu\text{M}$ , gave a secondary dissociation constant for (FKBP·rapamycin)·FRB of  $6.2$  nM ( $R^2 = 0.97$ , Figure 2B). Despite unanticipated difficulties in this experimental system, these data suggest that there are significant differences ( $\sim 1000$ -fold) between the affinities of rapamycin alone and the FKBP·rapamycin complex for FRB.

To validate both the fluorescence polarization method and the mathematical fits of the competition data to derive dissociation constants, the affinity of rapamycin for FKBP was determined using a competition binding assay (Figure 2C). The experiment was performed using FI-SLF (Fluorescein-labeled Synthetic Ligand for FKBP, Chart S1, Supporting Information) as a tracer.<sup>28</sup> FI-SLF was incubated with FKBP, along with various concentrations of rapamycin. The data were fit using the mathematical model, and the best fit gave a dissociation constant of  $0.35$  nM ( $R^2 = 0.96$ ). This value is similar to that measured by other methods,<sup>8</sup> validating the experimental method and the mathematical treatment of the data.

**Surface Plasmon Resonance.** The limited solubility of rapamycin precluded full characterization of its affinity for FRB using fluorescence polarization. As a result, we turned to surface plasmon resonance (SPR) as a complementary method to interrogate this system.<sup>29,30</sup> To validate SPR as a technique for interrogating these protein–ligand interactions, we first immobilized a GST-FKBP fusion protein to the modified dextran surface of a CM5 chip and exposed this surface to various concentrations of rapamycin. These experiments provided a dissociation constant for the FKBP·rapamycin interaction ( $K_d = 0.27$  nM, Figure S2, Supporting Information) that is nearly identical to both the literature value ( $K_d = 0.2$  nM)<sup>8</sup> and the affinity measured by fluorescence polarization ( $K_d = 0.35$  nM, Figure 2C).

In our initial studies of the rapamycin·FRB interaction, we sought to capture a GST-FRB fusion protein using an anti-GST antibody immobilized on the dextran surface. Using this format we could expose the FRB surface to various concentrations of rapamycin and quantitate the interactions. This experimental design would allow us to use a fresh protein surface for each titration point, making it unnecessary to expose FRB to harsh regeneration conditions between each injection of analyte. Additionally, the only modified species in the experiment would be the GST-FRB fusion protein. We have characterized this fusion protein using fluorescence polarization, and have shown that it has an affinity for FI-rap similar to that of the isolated FRB domain ( $K_d = 960 \pm 69$  nM vs  $K_d = 490 \pm 39$  nM, Figure S3, Supporting Information). Unfortunately, the titration could not be completed, again due to rapamycin's limited solubility in aqueous buffer. At high concentrations of rapamycin ( $>5 \mu\text{M}$ ), we observed irregularities in the sensorgrams that were indicative of a heterogeneous solution of analyte.

These results suggested that rapamycin would have to be immobilized in order to complete the binding isotherm. We first acylated the C40-cyclohexyl hydroxyl group with various protected glycine derivatives. However, unmasking the amino group led to rapid degradation of these derivatives. Therefore, we designed a biotin-rapamycin derivative containing an amino-hexanoic acid spacer (long chain, LC) between the two molecules to minimize possible interactions between the two proteins.<sup>31</sup> Biotin-LC-rapamycin (Chart 1) proved to be stable and displayed a high affinity for Neutravidin.

For all SPR experiments, we used various surface loading levels to allow for a more informed analysis of the resulting data fit. When determining dissociation constants, it is ideal for the concentration of the species being titrated to be at least an order of magnitude below that of the dissociation constant,<sup>32</sup> but with SPR, only an estimate of concentration on the surface can be made. To be sure of the accuracy of the data fit, the values measured across multiple loading levels and fitting parameters (kinetic vs equilibrium binding) can be compared.

Neutravidin is a deglycosylated version of avidin with a nearly neutral  $pI$  (6.3), which we used as a biotin-binding domain (Figure 3A) as it yields the lowest nonspecific binding among the known biotin-binding proteins. Neutravidin was immobilized

(29) Myszka, D. G. *Methods Enzymol.* **2000**, *323*, 325–340.

(30) Day, Y. S. N.; Baird, C. L.; Rich, R. L.; Myszka, D. G. *Protein Sci.* **2002**, *11*, 1017–1025.

(31) Wilchek, M.; Bayer, E. A. *Methods Enzymol.* **1990**, *184*, 123–138.

(32) Kenakin, T. *Pharmacologic Analysis of Drug–Receptor Interaction*, 3rd ed.; Lippincott-Raven: Philadelphia, PA, 1997; Chapter 8.



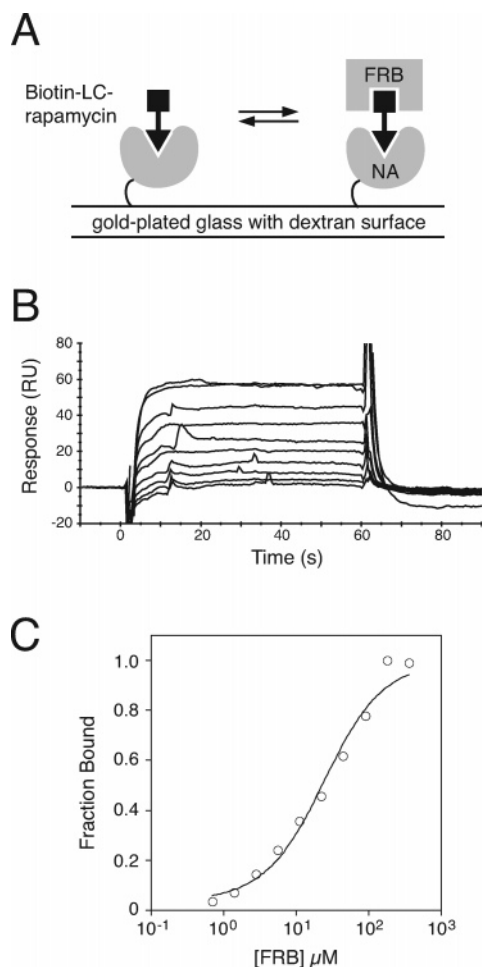


**Figure 3.** SPR analysis of the rapamycin•FRB interaction. (A) Schematic showing the experimental design (see text for details, NA = neutravidin). (B) A representative data set. Data shown is the response of the biotin-LC-rapamycin surface to various concentrations of FRB (0.7–360  $\mu\text{M}$ ). (C) Equilibrium binding analysis provides a rapamycin•FRB dissociation constant of  $26 \pm 0.8 \mu\text{M}$ .

using standard amine coupling on three active surfaces of a CM5 chip at loading levels of 250, 500, and 1000 RU. The final surface had an immobilization level of 1000 RU Neutravidin and served as the reference surface. The active surfaces were then saturated with biotin-LC-rapamycin (10, 55, and 95 RU, respectively), while the reference surface was saturated with biotinyl-6-aminohexanoic acid. Various concentrations of FRB were exposed to the surfaces, and a representative titration sensorgram is shown in Figure 3B. A qualitative analysis of the data shows characteristics of a micromolar interaction. The association and dissociation rates are too fast to be accurately measured by SPR, so we used an equilibrium binding analysis to determine the dissociation constant. The data were transferred into the BiaEvaluation software, and this analysis provided a dissociation constant of  $26 \pm 0.8 \mu\text{M}$  (Figure 3C).

We prepared a second biotin-rapamycin conjugate using a longer linker (Chart S2, Supporting Information) to determine if tethering rapamycin too close to the surface attenuated the affinity of FRB for the immobilized ligand. The dissociation constant between FRB and the longer biotin-rapamycin conjugate was found to be nearly identical to that of biotin-LC-rapamycin (23  $\mu\text{M}$  and 26  $\mu\text{M}$ , respectively, Figure S4, Supporting Information), suggesting that surface effects do not reduce the affinity of soluble FRB for the immobilized ligand.

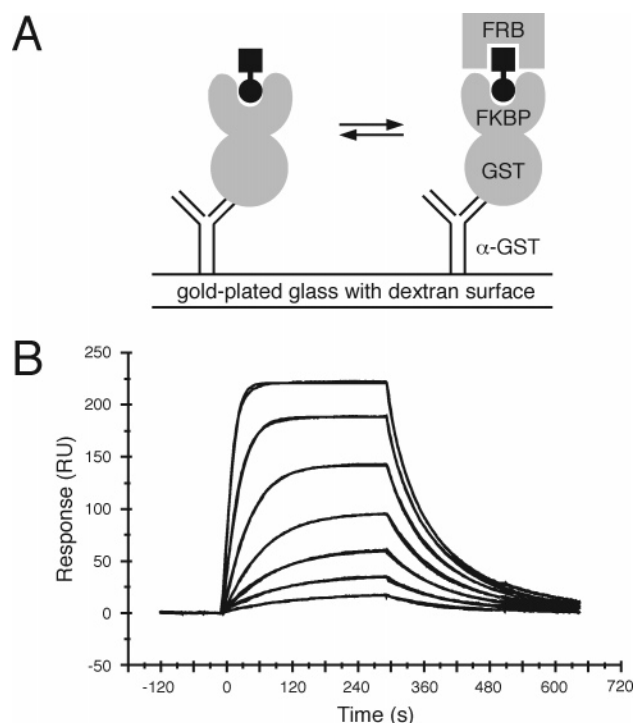


**Figure 4.** SPR analysis of the secondary dissociation constant of FRB for GST-FKBP•rapamycin. (A) Schematic showing the experimental design (see text for details). (B) A representative data set showing an overlay of both raw data and a kinetic fit for each FRB concentration. The GST-FKBP•rapamycin surface was exposed to various concentrations of FRB (1–60 nM). A kinetic fit of the data for four independent experiments provides an average dissociation constant of  $12 \pm 0.8 \text{ nM}$ .

We were able to use the GST-capture method described above to measure the affinity of FRB for the FKBP•rapamycin complex (Figure 4A). We prepared a GST-FKBP•rapamycin surface by first immobilizing an anti-GST antibody through standard amine coupling to the dextran surface. Various levels of GST-FKBP fusion protein were captured on active flow cells, and matching levels of GST were captured on the reference flow cells. The FKBP domains were then saturated with rapamycin using 50 nM rapamycin in all buffers. Given the dissociation constants of rapamycin for FKBP and FRB ( $K_d = 0.2 \text{ nM}$  and  $K_d = 26 \mu\text{M}$ , respectively), this concentration ensures that all FKBP binding domains are saturated, while rapamycin•FRB complexation is negligible. Finally, various concentrations of FRB, all with 50 nM rapamycin, were exposed to the surface, and a representative sensorgram is shown in Figure 4B. The titration was performed to saturation, but data points from both high and low concentrations of analyte have been omitted for clarity.

A kinetic fit of the data shows that formation of trimeric complex is quite favorable, with a dissociation constant of  $12 \pm 0.8 \text{ nM}$  ( $k_a = 1.92 \times 10^6 \text{ M}^{-1}\text{s}^{-1}$ ,  $k_d = 2.2 \times 10^{-2} \text{ s}^{-1}$ ). Thus, presentation of rapamycin by FKBP provides an  $\sim 2000$ -fold enhancement over the affinity of rapamycin alone for FRB. An additional data set allowed for both an equilibrium binding analysis and a kinetic fit of the data, with identical results (Figure S5, Supporting Information).

It has been previously shown that when the C16-methoxy group of rapamycin is replaced with a bulky trimethoxyphenyl group (TMOP-rapamycin, Chart 1), the activity of the FKBP•TMOP-rapamycin complex in several biological assays is

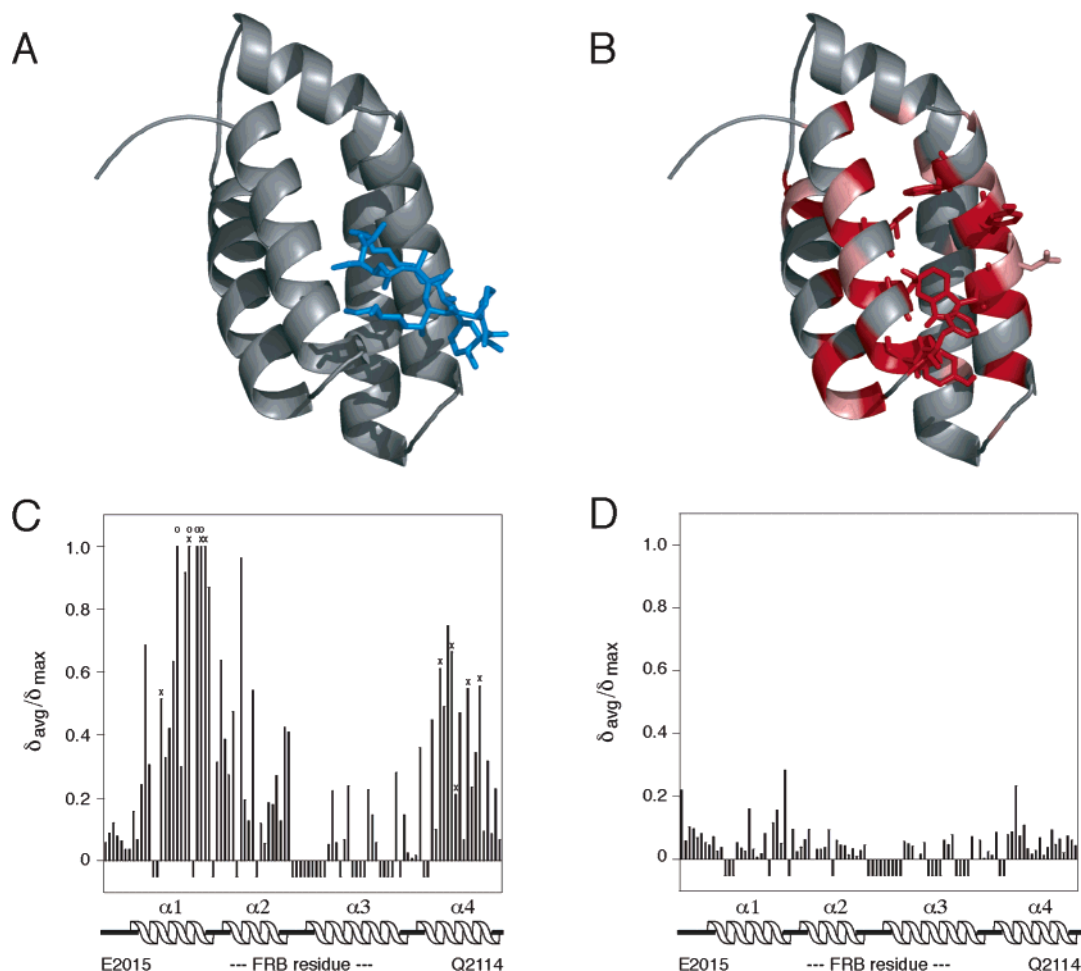


**Figure 5.** Effects of rapamycin and TMOP-rapamycin titrations on backbone  $^1\text{H}$  and  $^{15}\text{N}$  chemical shifts of FRB. Perturbations are displayed as normalized weighted average shift differences,  $\delta_{\text{avg}}/\delta_{\text{max}}$  (see Experimental Procedures). All experiments are normalized with respect to the residue that showed the greatest perturbation in chemical shift (F2039) from the rapamycin·FRB titration. Unassigned resonances are indicated as such by a negative chemical shift difference. Ribbon representations were created using PyMOL.<sup>37</sup> (A) Ribbon representation of FRB showing the rapamycin binding site (adopted from the FKBP·rapamycin·FRB crystal structure, 1FAP).<sup>24</sup> Rapamycin is shown in blue. (B) FRB ribbon representation showing residues affected by the rapamycin titration. Side chains of residues that make van der Waals contacts with rapamycin are shown. Residues experiencing strong chemical shift perturbations ( $\delta_{\text{avg}}/\delta_{\text{max}} > 0.4$ ) are shown in red and residues experiencing moderate chemical shift perturbations ( $0.2 < \delta_{\text{avg}}/\delta_{\text{max}} < 0.4$ ) are shown in pink. Rapamycin has been omitted for clarity. (C) Chemical shift perturbations for the rapamycin·FRB titration are plotted as a function of residue number. Residues that make van der Waals contacts with rapamycin (L2031, S2035, Y2038, F2039, W2101, Y2105, and F2108) are indicated as such ( $\times$ ). The resonances for E2032, S2035, L2037, and Y2038 (denoted with an  $\circ$ ) broaden and become unobservable upon addition of rapamycin. These four residues have been assigned a value of 1. Secondary structure is indicated at the bottom of the graph. (D) Chemical shift perturbations for the TMOP-rapamycin·FRB titration are plotted as a function of residue number.

reduced by at least 3 orders of magnitude, whereas the activity of TMOP-rapamycin in a rotamase inhibition assay is decreased only modestly.<sup>33</sup> These results suggest that TMOP-rapamycin retains its ability to bind to FKBP, but can no longer bind to FRB because of unfavorable steric interactions. To demonstrate the specificity of the rapamycin·FRB interactions, we repeated the experiment described above, substituting the rapamycin in the buffer with TMOP-rapamycin. As expected, the response levels observed from this titration are extremely low (data not shown), demonstrating that the response observed upon FRB titration is specific to the FKBP·rapamycin surface.

The affinity of the FKBP·rapamycin complex for FRB is approximately 2000-fold tighter than the affinity of rapamycin alone for FRB. This observation suggests that protein-protein

interactions between FKBP and FRB contribute to the overall stability of the ternary complex. To test this hypothesis, we sought evidence of these interactions in the absence of rapamycin. GST-FKBP was captured on an active flow cell, and a matching level of GST was captured on the reference flow cell. The FKBP surface was exposed to  $5\ \mu\text{M}$  FRB with no response observed (data not shown), suggesting that the dissociation constant between FKBP and FRB is no lower than  $50\ \mu\text{M}$ .

**NMR Binding Assay.** Chemical shifts are sensitive to local chemical environment, and perturbations in chemical shift upon titration are a good indication that two species are interacting. As additional evidence of the specificity of the rapamycin·FRB interaction in the absence of FKBP, we used NMR spectroscopy to monitor changes in chemical environment of FRB residues upon complexation with rapamycin.

We used  $^1\text{H}/^{15}\text{N}$  HSQC spectra to monitor rapamycin·FRB interactions, but first, we wanted to correlate the individual HSQC resonances with specific residues within FRB. Three-

(33) Luengo, J. I.; Yamashita, D. S.; Dunnington, D.; Beck, A. K.; Rozamus, L. W.; Yen, H.-K.; Bossard, M. J.; Levy, M. A.; Hand, A.; Newman-Tarr, T.; Badger, A.; Faucette, L.; Johnson, R. K.; D'Alessio, K.; Porter, T.; Shu, A. Y. L.; Heys, R.; Choi, J.; Kongsaree, P.; Clardy, J.; Holt, D. A. *Chem. Biol.* **1995**, *2*, 471–481.

dimensional NMR experiments were performed and analyzed using uniformly  $^{13}\text{C}/^{15}\text{N}$ -labeled FRB. Sample instability at the higher concentrations necessary for 3D analysis by NMR in addition to the flexibility of the  $\alpha 3$  helix impacted the quality of data acquired; however, a sequential assignment of 80% of the FRB backbone was obtained (supplementary data).

Using uniformly  $^{15}\text{N}$ -labeled FRB, we monitored changes in the amide chemical shifts of FRB as a function of rapamycin concentration using  $^1\text{H}/^{15}\text{N}$  HSQC spectra.<sup>34–36</sup> An FRB sample (100  $\mu\text{M}$  FRB in 20 mM PBS pH 6.8, 10%  $\text{D}_2\text{O}$ ) was treated with substoichiometric amounts of rapamycin (0.125 equiv) up to a 1:1 ratio of rapamycin to FRB, and then in 0.5 equiv increments to a final 2:1 ratio of rapamycin to FRB. HSQC spectra were obtained for each titration point, and the spectra were compared to monitor chemical shift perturbations.

The amide resonances of FRB displayed a range of behaviors during the rapamycin titration, with peaks in fast, slow, and intermediate exchange with respect to the NMR time scale. Given the micromolar affinity of rapamycin for FRB, we might expect that residues directly involved in a binding event would exhibit slow exchange behavior. Our analysis of the rapamycin•FRB complex showed that residues that make van der Waals contacts with rapamycin (L2031, S2035, Y2038, F2039, W2101, Y2105, and F2108)<sup>24,25</sup> are all either in slow exchange or are broadened to such an extent upon binding that the resonances are no longer observable.

The existence of the FKBP•rapamycin•FRB crystal structure<sup>24,25</sup> coupled with our sequential assignment of FRB allowed us to correlate chemical shift changes upon rapamycin binding for 79 of 102 residues (Figure 5A–C). Figure 5A shows the FKBP•rapamycin•FRB crystal structure, highlighting the rapamycin-binding site. Figure 5B shows FRB in the same orientation. Rapamycin has been removed for clarity, and side chains that make van der Waals contacts with rapamycin are explicitly shown. Residues greatly affected by the rapamycin titration are shown in red, and those moderately affected are shown in pink. Chemical shift perturbations were then plotted as a function of FRB sequence (Figure 5C). All residues known to be involved in rapamycin binding were affected by rapamycin titration, and the residues most affected by the titration lie along helices  $\alpha 1$  and  $\alpha 4$ , the crossing of which forms the rapamycin binding pocket.<sup>24</sup>

NMR experiments must be performed at relatively high concentrations, so we were mildly concerned that these high protein concentrations might lead to aggregation, exposing hydrophobic surfaces that might interact with rapamycin non-specifically. If rapamycin is simply binding to hydrophobic areas of FRB, TMOP-rapamycin might be expected to exhibit the same behavior. Conversely, if rapamycin is making specific contacts with FRB, TMOP-rapamycin should be excluded from this interaction for steric reasons. To ensure that the observed chemical shift perturbations were due to a specific rapamycin•FRB interaction, we repeated the  $^1\text{H}/^{15}\text{N}$  HSQC titration using TMOP-rapamycin, with little perturbation in chemical shift observed (Figure 5D). Upon addition of 1.0 equiv of rapamycin

to this mixture of FRB and TMOP-rapamycin, chemical shift perturbations similar to those observed at 1:1 rapamycin:FRB complex were observed (Figure S6, Supporting Information), showing the specificity of the rapamycin•FRB interaction.

Our SPR results suggest that any interaction between FKBP and FRB in the absence of rapamycin is weak ( $K_d \geq 50 \mu\text{M}$ ). We took advantage of NMRs ability to measure dissociation constants in this range in an attempt to obtain a more quantitative analysis.  $^1\text{H}/^{15}\text{N}$  HSQC titration was performed in which 100  $\mu\text{M}$   $^{15}\text{N}$ -labeled FRB was titrated with FKBP in concentrations up to 1 mM (data not shown). Even at these high protein concentrations little perturbation in chemical shift was observed. This finding suggests that FKBP and FRB do not appreciably associate in the absence of rapamycin, despite the stabilizing effects of protein–protein interactions at the interface of the FKBP•rapamycin•FRB ternary complex.

## Conclusions

We have used fluorescence polarization, surface plasmon resonance, and NMR spectroscopy to characterize the intermolecular interactions involved in the formation of the FKBP•rapamycin•FRB ternary complex. Of these four possible interactions (Figure 1B), only the FKBP•rapamycin interaction had been previously characterized, and our measurements using two independent techniques are in agreement with the literature value ( $K_d = 0.2 \text{ nM}$ ).<sup>8</sup> The affinity of rapamycin for FRB in the absence of FKBP is modest ( $K_d = 26 \pm 0.8 \mu\text{M}$ ), and a 2000-fold improvement is observed in the presence of FKBP ( $K_d = 12 \pm 0.8 \text{ nM}$ ). On the basis of these measurements, one would predict the affinity of the rapamycin•FRB complex for FKBP to be 100 fM. Although they appear to contribute significantly to the stability of the ternary complex, protein–protein interactions between FKBP and FRB in the absence of rapamycin were not observed.

These results suggest that the FKBP•rapamycin complex is most likely the biologically relevant ligand for mTOR, as rapamycin alone would not bind appreciably to mTOR under physiological conditions. While FKBP is necessary for rapamycin to bind to mTOR, these data do not rule out the possibility that FKBP acts in an additional capacity to sterically block interactions between mTOR and a functionally relevant protein (i.e., substrate or signaling partner), with rapamycin modulating this activity. The dramatic difference between the dissociation constants of rapamycin alone and the FKBP•rapamycin complex for FRB suggests that protein–protein interactions at the FKBP–FRB interface play a critical role in stabilizing the ternary complex. A thorough analysis of the individual residues at the FKBP–FRB interface will likely provide a more quantitative and complete understanding of the individual contributions to the stability of the ternary complex.

## Experimental Procedures

**Fluorescence Polarization Binding Assays. (i) Saturation Binding Experiments.** The affinity of Fl-rap for FRB was determined as follows. Fl-rap (2 nM) was incubated with various concentrations of purified recombinant FRB (4 nM to 34  $\mu\text{M}$ ) in PBS pH 7.4, 0.011% Triton X-100, 0.1 mg/mL bovine  $\gamma$ -globulin (BGG). Polarization units (mP) were plotted against FRB concentration and fit in Kaleidagraph using the equation  $F_0 - (F_0 - F_\infty)(K_d + [\text{tracer}]_{\text{total}} + \mathcal{J}) - ((K_d + [\text{tracer}]_{\text{total}} + \mathcal{J})^2 - 4([\text{tracer}]_{\text{total}} \mathcal{J}))^{0.5} / (2([\text{tracer}]_{\text{total}}))$ , where  $F_0$  is the polarization of free fluorescent tracer,  $F_\infty$  is the polarization of bound

(34) Bodenhausen, G.; Ruben, D. J. *Chem. Phys. Lett.* **1980**, *69*, 185–189.

(35) Kay, L. E.; Keifer, P.; Saariinen, J. T. *J. Am. Chem. Soc.* **1992**, *114*, 10663–10665.

(36) Shuker, S. B.; Hajduk, P. J.; Meadows, R. P.; Fesik, S. W. *Science* **1996**, *274*, 1531–1534.

(37) DeLano, W. L. *The PyMOL Molecular Graphics System*; DeLano Scientific: San Carlos, CA, 2002 (<http://www.pymol.org>).



tracer,  $[\text{tracer}]_{\text{total}}$  is the total tracer concentration, and  $\mathcal{P}$  is the measured polarization at each protein concentration.

**(ii) Competition Binding Experiments.** The affinity of rapamycin for FRB was determined as follows. Fl-rap (10 nM) was incubated with FRB (1  $\mu\text{M}$ ) in PBS pH 7.4, 0.011% Triton X-100, 0.1 mg/mL BGG, along with various concentrations of rapamycin (14 nM to 10  $\mu\text{M}$ ). Polarization units were converted to fraction bound tracer and plotted against rapamycin concentration. The data were then fit using a quantitative mathematical model.<sup>28</sup> The best data fit was determined by  $R^2$  value.

The affinity of rapamycin for FKBP was determined as follows. Fl-SLF (0.5 nM) was incubated with FKBP (5 nM) in PBS pH 7.4, 0.011% Triton X-100, 0.1 mg/mL BGG, along with various concentrations of rapamycin (0.05–100 nM). Polarization units were converted to fraction bound tracer and plotted against rapamycin concentration. The data were then fit using a quantitative mathematical model.<sup>28</sup> The best data fit was determined by  $R^2$  value.

**(iii) Competition Binding Experiments with Presenter Protein.** The affinity of FKBP·rapamycin for FRB was determined as follows. Fl-rap (10 nM) was incubated with FRB (1  $\mu\text{M}$ ) and FKBP (1  $\mu\text{M}$ ) in PBS pH 7.4, 0.011% Triton X-100, 0.1 mg/mL BGG, along with various concentrations of rapamycin (1.4 nM to 1  $\mu\text{M}$ ). Polarization units were converted to fraction bound tracer and plotted against rapamycin concentration. The data were then fit using quantitative mathematical model.<sup>28</sup> The best data fit was determined by  $R^2$  value.

**Surface Plasmon Resonance Assays.** Surface plasmon resonance measurements were performed at 25 °C using a Biacore 3000. All buffers were filtered and degassed for 20 min. When changing buffers, the system was equilibrated in the new buffer (primed 5 $\times$ ) before use. All data were reference subtracted against both the reference flow cell and a buffer injection. Kinetic data were fit to  $dR/dt = k_a C(R_{\text{max}} - R_{\text{obs}}) - k_d R_{\text{obs}}$ , where  $C$  is the analyte concentration.

**(i) Affinity of Biotin–LC–Rapamycin for FRB.** Neutravidin was diluted in immobilization buffer (10  $\mu\text{g}/\text{mL}$  in 10 mM sodium acetate, pH 5.0) and immobilized onto three flow cells of a CM5 chip at 250, 500, and 1000 RU. Neutravidin (1000 RU) was immobilized on the final flow cell, which served as the reference surface. Biotin-LC-rapamycin was diluted into the running buffer (10  $\mu\text{g}/\text{mL}$  in PBS pH 7.4, 0.002% Tween-20), and the three active flow cells were saturated with this conjugate (10, 55, and 95 RU, respectively). The reference cell was saturated with biotinyl-aminohexanoic acid. Various concentrations of FRB (0.7–360  $\mu\text{M}$ ) were injected over the surface (50  $\mu\text{L}/\text{min}$ , 50  $\mu\text{L}$  injection with 120 s wash delay). The surface was regenerated between analyte injections with 35% EtOH (40  $\mu\text{L}$  at 20  $\mu\text{L}/\text{min}$ ). The data were transferred into BiaEvaluation and fit using an equilibrium binding analysis.

**(ii) Affinity of GST–FKBP·Rapamycin for FRB.** Approximately 20 000 RU anti-GST antibody was immobilized on all four flow cells of a CM5 chip using traditional amine coupling chemistry. GST-FKBP was diluted into the running buffer (10  $\mu\text{g}/\text{mL}$  in PBS pH 7.4, 0.002% Tween-20, 50 nM rapamycin) and captured individually on two of the antibody surfaces, at densities of 500 and 1000 RU, respectively. On the remaining two antibody surfaces, 500 and 1000 RU of GST were individually captured to give the corresponding reference surfaces. Various concentrations of FRB (6 pM to 1  $\mu\text{M}$ ) were exposed to the GST-FKBP·rapamycin active surface and the GST reference surface at a flow rate of 50  $\mu\text{L}/\text{min}$  (250  $\mu\text{L}$  injection, 300 s wash delay). The surface was regenerated between analyte injections with 10 mM glycine

pH 2.2 (40  $\mu\text{L}$  at 20  $\mu\text{L}/\text{min}$ ). The BiaEvaluation software program was used for data fitting.

**NMR Spectroscopy.**  $^1\text{H}/^{15}\text{N}$  HSQC two-dimensional spectra for the rapamycin/FRB titration (described below) were acquired on a Varian 800 MHz Inova spectrometer.  $^{15}\text{N}$ –NOESY–HSQC, HNCACB, and CBCACONH three-dimensional spectra were acquired on  $^{13}\text{C}/^{15}\text{N}$ –FRB (600  $\mu\text{M}$  in 250  $\mu\text{L}$  in Shigemi symmetrical microtube, 20 mM PBS pH 6.8, 10%  $\text{D}_2\text{O}$ ) on Varian 600 and 800 MHz Inova spectrometers. All experiments were acquired at 25 °C, and both spectrometers were running VNMR v6.1C. Spectra were processed with VNMR and analyzed utilizing Sparky.<sup>38</sup>

**NMR Titration of Rapamycin into FRB.** A sample of  $^{15}\text{N}$ –FRB (500  $\mu\text{L}$ , 100  $\mu\text{M}$ ) was prepared in NMR buffer (20 mM PBS pH 6.8, 10%  $\text{D}_2\text{O}$ ) and a  $^1\text{H}/^{15}\text{N}$  HSQC spectrum of the free protein was acquired. Rapamycin (1  $\mu\text{L}$  of a 6.25 mM stock in ethanol, 0.125 equiv) was added, and after 20 min incubation, an HSQC spectrum was acquired. Rapamycin was added in 0.125 equiv aliquots (1  $\mu\text{L}$ ) up to 1.0 molar equiv with respect to FRB, and then two final additions (1  $\mu\text{L}$  of a 25 mM stock, 0.5 equiv) were performed to achieve a final 2:1 ratio of rapamycin to FRB (total ethanol concentration of 2%). HSQC spectra were acquired and analyzed for each titration point. A control experiment using TMOP-rapamycin was performed in the same manner, with an addition of 1.0 equiv of rapamycin (2  $\mu\text{L}$  of a 25 mM stock) as the final titration point. All experiments were performed at 25 °C.

**Chemical Shift Perturbation.** The  $^1\text{H}/^{15}\text{N}$  HSQC spectrum of FRB complexed with rapamycin was compared with that of free FRB. To evaluate the effects, the normalized weighted average shift difference of the  $^1\text{H}$  and  $^{15}\text{N}$  resonances,  $\delta_{\text{avg}}/\delta_{\text{max}}$ , for each residue was calculated. The weighted average shift difference,  $\delta_{\text{avg}}$ , was calculated as  $\{[\delta_{\text{H}}^2 + (\delta_{\text{N}}^2/5)]/2\}^{1/2}$ , where  $\delta_{\text{H}}$  and  $\delta_{\text{N}}$  are the change in ppm between free and bound chemical shifts.  $\delta_{\text{max}}$  was set to be the maximum observed weighted average shift difference.<sup>39</sup> All experiments were normalized with respect to  $\delta_{\text{max}}$  from the rapamycin·FRB titration series.

**Acknowledgment.** L.A.B. and T.J.W. thank the NIH (GM-068589) and NSF (CHE-9985214) for funding of this work. C.W.L. and the Stanford Magnetic Resonance Laboratory are funded in part by the Stanford University School of Medicine. We thank Professor Jie Chen for the pGEX-FKBP and pGEX-FRB plasmids. We thank Professor Carolyn Bertozzi for use of the Biacore 3000. We thank Dr. Patrick Braun and Professor Jody Puglisi for helpful discussions.

**Supporting Information Available:** Supporting figures; experimental details for the synthesis of rapamycin derivatives and spectra of the compounds; partial differential equations used to fit competition binding data for dissociation constants; additional details regarding SPR experiments; chemical shift assignments for FRB backbone residues. This material is available free of charge via the Internet at <http://pubs.acs.org>.

JA043277Y

(38) Goddard, T. D.; Kneller, D. G. *SPARKY 3*; University of California: San Francisco, 2002.

(39) Garrett, D. S.; Seok, Y. J.; Peterofsky, A.; Clore, G. M.; Gronenborn, A. M. *Biochemistry* **1997**, *36*, 4393–4398.